Hui et al. 2015. *Int. J. Vehicle Structures & Systems*, 7(2), 55-60
ISSN: 0975-3060 (Print), 0975-3540 (Online)
doi: 10.4273/ijvss.7.2.02

International Journal of Vehicle Structures & Systems
Available online at www.maftree.org/eja

Vertical Vibration Analysis of the Flexible Carbody of High Speed Train

Cao Hui[a,b], Zhang Weihua[a] and Miao Bingrong[a]

[a]*Traction Power State Key Laboratory, Southwest Jiaotong University, Chengdu, China*

[b]*School of Mfg. Science and Engg., Southwest University of Science & Technology, Mianyang, China*
Corresponding Author, Email: ch_hello@163.com

ABSTRACT:

The elastic vibrations in carbody affect the safety of suspension components and the riding comfort of high speed trains. The vertical vibration of a carbody was studied based on a coupled rigid-flexible dynamic model. The vibration characteristics and the transfer relationship under flexible effect were investigated in frequency domain. Analysis results show that the symmetrical and non-symmetric mode responses achieve maximum in specific wavelengths. The resonance speed and resonance wavelength of the first-order vertical bending vibration have significant impact on the operation of the train. When the modal frequencies of the carbody are equal to the natural frequencies, the carbody produces modal resonance. Therefore, high first-order bending frequency improves the safety and the riding comfort.

KEYWORDS:

High speed train; Flexible carbody; Dynamic model; Suspension parameters

CITATION:

C. Hui, Z. Weihua and M. Bingrong. 2015. Vertical Vibration Analysis of the Flexible Carbody of High Speed Train, *Int. J. Vehicle Structures & Systems*, 7(2), 55-60. doi:10.4273/ijvss.7.2.02.

1. Introduction

Speed and comfort are the core competiveness for high-speed trains when compared with other transports. The carbody is increasingly lighter in weight. With the increasing train speed, the track excitation frequency is increased. This leads to more flexibility and reduces the modal frequency. This could cause serious vibrations in a frequency range to which passengers aboard train are very sensitive, thus affects the ride comfort. This vibration also causes carbody fatigue which affects the dynamic performance and service life of the vehicle [1-3]. In order to improve the performance of the vehicle vertical dynamics, several methods were already proposed. The dynamic vibration absorber and flexible damper are installed under carbody and the control effects are analyzed by absorber parameters and installation style [4-6]. Zeng et al [7] designed appropriate constrained damping layers to obtain good damping effect. A novel method for vibration reduction is the application of an active control system directly to the flexible structure of the railway carbody to attenuate the elastic vibrations.

Both passive and active control schemes have already been proposed by Huang et al [8]. Above research focussed on the factors and measures of improvement in ride quality under the elastic body structure. The research on the vibration mechanisms and transfer relationship under flexibility effect is limited. In this paper, a vertical dynamics model for high-speed train was established based on rigid-flexible coupled dynamics. Resonance effect and filtering effect exist in elastic vibrations. The factors influencing vibrations and ride comfort are analyzed.

2. Rigid-flexible coupled dynamics model

The vertical rigid-flexible coupled dynamics model for high speed train is as shown in Fig. 1. The model includes carbody, bogie, wheelsets and suspensions. The carbody is modelled as a simple Euler-Bernoulli beam in consideration of only vertical vibration, i.e., bounce, pitching and bending modes. The wheelsets and bogie frames are considered as rigid bodies. The pitching motion of bogie frame is neglected as it is independent in the vehicle vertical system. As a result, the total number of independent degrees of freedom of the rigid vehicle system is four, namely front frame bounce z_{b1}, rear frame bounce z_{b2}, carbody bounce z_{c3}, and carbody pitching θ_c. When n flexible modes are considered, the n modal coordinate can deem the flexible vibration freedom. So, the total degrees of freedom is 4+n. The parameters of typical high speed passenger train are shown in Table 1.

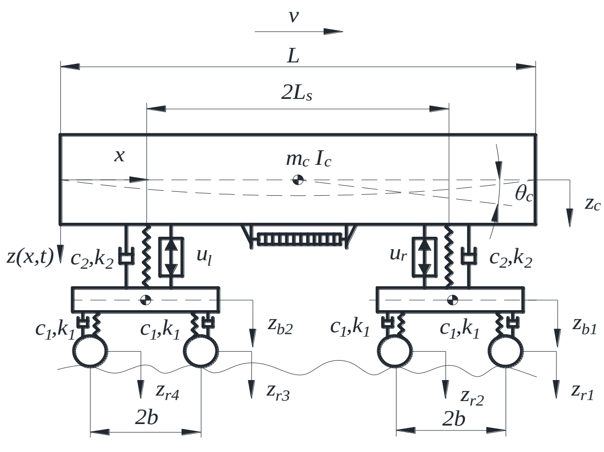

Fig. 1: Dynamic model of vehicle system

Table 1: Parameters of vehicle dynamics model

Parameter description	Symbol	Value
Mass of carbody	m_c (t)	26
Carbody pitch inertia	I_c (tm^2)	1300
Mass per meter	ρA (tm^{-1})	1.07
Bending rigidity	EI (kN/m^2)	3.58×10^6
Bogie frame mass	m_b (t)	2.44
Bogie frame pitch inertia	I_b (tm^2)	1.4
Primary damping coeff. per axle	c_1 (kNs/m)	30
Sec. damping coeff. per bogie	c_2 (kNs/m)	50
Primary spring coeff. per axle	k_1 (kN/m)	2400
Sec. spring coefficient per bogie	k_2 (kN/m)	380
Length of carbody	L (m)	24.5
Half of bogie centres	L_s (m)	8.75
1st bending mode frequency	f_1	10.02
1st bending mode damping ratio	ξ_1	1.5%
2nd bending mode frequency	f_2	27.83
2nd bending mode damping ratio	ξ_2	1.5%

When the vertical displacement of carbody being expressed as *u(x, t)*, the appropriate partial differential equation of the carbody is given by [1],

$$EI\frac{\partial^4 u(x,t)}{\partial x^4}+\rho A\frac{\partial^2 u(x,t)}{\partial t^2}+\phi I\frac{\partial^5 u(x,t)}{\partial x^4\partial t} = \sum_{i=1}^{2}F_i\delta(x-x_i) \tag{1}$$

Where x_i is the second suspension displace, i=1 means front bogie and i=2 means rear one. $\delta(x)$ is the delta function. F_i is the forces acted by second suspensions and are given by,

$$F_i=-c_2[\dot{u}(x_i,t)-\dot{z}_{bi}]+k_2[u(x_i,t)-z_{bi}] \tag{2}$$

It is assumed that the shape function and modal coordinate of i^{th} mode are $Y_i(x)$ and $q_i(t)$ respectively. When the rigid modes are included with the flexible modes in $z(x,t)$, the first mode of the carbody is chosen as the bounce of rigid mode and its shape function is taken as $Y_1(x)$=1. The second mode is the pitch and its shape function is $Y_1(x)=L/2-x$ accordingly under the coordinate system definition as in Fig. 1. When N modes are considered, the vertical displacement of the carbody can be written as,

$$u(x,t)=z_c(t)+(x-L/2)\theta_c(t)+\sum_{i=3}^{N}Y_i(x)q_i(t) \tag{3}$$

The shape functions are taken as,

$$Y_i(x)=ch\beta_i x+\cos\beta_i x-\frac{ch\beta_i L+\cos\beta_i L}{Sh\beta_i L+\sin\beta_i L}(sh\beta_i x+\sin\beta_i x) \tag{4}$$

Where $\beta_i=(2i+1)\pi/(2L)$. By substituting Eqn. (3) into Eqn. (1) and integrating along the length of carbody, considering the orthogonality of shape functions, the carbody and bogies vibration equations are given by,

$$\begin{aligned}
&\ddot{q}_i(t)+2\xi_1\omega_i\dot{q}_i+\omega_i^2 q_i=\frac{Y_i(x_1)}{m_c}F_1+\frac{Y_i(x_2)}{m_c}F_2;\\
&m_c\ddot{z}(t)=\sum_{i=1}^{2}F_i;\quad I_c\ddot{\theta}(t)=\sum_{i=1}^{2}F_i(x_i-L/2);\\
&m_b\ddot{z}_{b1}+c_2[\dot{z}_{b1}-\dot{u}(x_1,t)]+k_2[z_{b1}-u(x_1,t)]\\
&\quad+c_1(2\dot{z}_{b1}-\dot{z}_{r1}-\dot{z}_{r2})+k_1(2z_{b1}-z_{r1}-z_{r2})=0;\\
&m_b\ddot{z}_{b2}+c_2[\dot{z}_{b2}-\dot{u}(x_2,t)]+k_2[z_{b1}-u(x_2,t)]\\
&\quad+c_1(2\dot{z}_{b2}-\dot{z}_{r3}-\dot{z}_{r4})+k_1(2z_{b2}-z_{r3}-z_{r4})=0\\
&I_b\ddot{\theta}_{b1}+c_1 b[2b\dot{\theta}_{b1}-\dot{z}_{r1}+\dot{z}_{r2}]\\
&\quad+k_1 b[2b\theta_{b1}-z_{r1}+z_{r2}]=0\\
&I_b\ddot{\theta}_{b2}+c_1 b[2b\dot{\theta}_{b2}-\dot{z}_{r3}+\dot{z}_{r4}]\\
&\quad+k_1 b[2b\theta_{b2}-z_{r3}+z_{r4}]=0
\end{aligned} \tag{5}$$

Where $\omega_i^2=EI\beta_i^4/\rho$, $2\xi_i\omega_i=\phi I\beta_i^4/\rho$. For the case of,

$$\{z\}=\{z_c\theta_c z_{b1}z_{b2}\theta_{b1}\theta_{b2}q_3.....q_N\}^T \tag{6}$$

Writing Eqns. (5) in matrix form gives

$$[M]\{\ddot{z}\}+[C]\{\dot{z}\}+[K]\{z\}=[C_r]\{\dot{z}_r\}+\{K_r\}\{z_r\} \tag{7}$$

In which [M], [K] and [C] are the inertia, stiffness, and damping matrices respectively. [C_r] and [K_r] are the speed input matrices and track displacement.

According to Eqn. (7), the FRF matrix H(ω), $H_a(\omega)$ of the carbody displacement and acceleration can be obtained by,

$$\begin{aligned}
&H(\omega)=[-\omega^2 M+j\omega C+K]^{-1}[-j\omega C_r+K_r]\\
&H_a(\omega)=-\omega^2 H(\omega)
\end{aligned} \tag{8}$$

Matrices obtained by Eqns. (8) are the multiple input multiple output (MIMO) displacement and acceleration FRF matrices, whose elements are the single input single output (SISO) FRFs from the single wheelsets to the carbody response, which do not include the time delay effect between wheelsets. For the vehicle dynamic model in Fig. 1, the track inputs vector is,

$$\{z_r(t)\}=\begin{Bmatrix}z_{r1}(t)\\z_{r2}(t)\\z_{r3}(t)\\z_{r4}(t)\end{Bmatrix}=\begin{Bmatrix}z_{r1}(t)\\z_{r1}(t-\tau_1)\\z_{r1}(t-\tau_2)\\z_{r1}(t-\tau_3)\end{Bmatrix} \tag{9}$$

Where $\tau_1=2b/V$,. $\tau_2=2L_s/V$,. $\tau_3=2(b+L_s)/V$. By Fourier transformations, the above equation one has

$$\{Z_r(\omega)\}=\{1\quad e^{-j\omega\tau_1}\quad e^{-j\omega\tau_2}\quad e^{-j\omega\tau_3}\}^T Z_{r1}(\omega) \tag{10}$$

Therefore, the system displacement responses in the frequency domain are:

$$\{Z_r(\omega)\}=H(\omega)\{1\quad e^{-j\omega\tau_1}\quad e^{-j\omega\tau_2}\quad e^{-j\omega\tau_3}\}^T Z_{r1}(\omega) \tag{11}$$

By assuming,

$$\begin{aligned}
&\{H_c(\omega)\}=H(\omega)\{1\quad e^{-j\omega\tau_1}\quad e^{-j\omega\tau_2}\quad e^{-j\omega\tau_3}\}^T\ \{H_{ac}(\omega)\}\\
&\quad=H_a(\omega)\{1\quad e^{-j\omega\tau_1}\quad e^{-j\omega\tau_2}\quad e^{-j\omega\tau_3}\}^T
\end{aligned} \tag{12}$$

$H_c(\omega)$ and $H_{ac}(\omega)$ become the displacement and acceleration single input multiple outputs (SIMO) FRFs from track input to vehicle responses. As these SIMO FRFs include time delay effects between wheelsets, they are called correlated FRF matrices [10].

The PSDs of vehicle displacement and acceleration responses can be obtained by,

$$\begin{aligned}
&S_z(\omega)=H_c^*(\omega)S_\omega(\omega,V)H_c^T(\omega)\\
&S_z(\omega)=H_{ac}^*(\omega)S_\omega(\omega,V)H_{ac}^T(\omega)
\end{aligned} \tag{13}$$

In which $H_c^*(\omega)$, $H_c^T(\omega)$ are the conjugation and simple transpose of the FRF matrix $H_c(\omega)$. $S_\omega(\omega,V)$ is the displacement response PSD matrices at running speed V.

3. Flexible carbody vibration analysis

In carbody rigid and flexible vibration, the shape functions can be divided into symmetric and anti-symmetric modes. The bounce, first bending and third bending functions are symmetric modes. The pitch, second bending and fourth bending functions are anti-symmetric modes. The displacement amplitude of FRF of symmetric and anti-symmetric modes are given by:

$$\begin{aligned} \left|H_c^S(\omega)\right| &= \left|2H^S(\omega)\right|\sqrt{(1+\cos\omega\tau_1)(1+\cos\omega\tau_2)} \\ \left|H_c^{AS}(\omega)\right| &= \left|2H^{AS}(\omega)\right|\sqrt{(1+\cos\omega\tau_1)(1-\cos\omega\tau_2)} \end{aligned} \quad (14)$$

For symmetric modes, when the wavelength of track irregularity input is,

$$\lambda = 4b/(2n-1) \text{ or } \lambda = 4L_s/(2n-1),\ n=1,2,3,... \quad (15)$$

then carbody response is zero. The corresponding frequencies are:

$$f = V(2n-1)/(4b) \text{ or } f = V(2n-1)/(4L_s) \quad (16)$$

Similarly, for anti-symmetric modes, the wavelength and frequency of carbody response are:

$$\lambda = 4b/(2n-1) \text{ or } \lambda = 2L_s/n,\ n=1,2,3,...$$

$$f = V(2n-1)/(4b) \text{ or } f = Vn/(2L_s),\ n=1,2,3,... \quad (17)$$

According to Eqns. (16) and (17), there will be no response when $f = V(2n-1)/(4b)$. Therefore, this is called as the filtering phenomenon. For symmetric modes, if the wavelengths of track irregularity input is,

$$\lambda = 2b/n \text{ or } \lambda = 2L_s/n,\ n=1,2,3,... \quad (18)$$

Then there will be maximum carbody responses. These are called symmetric resonance wavelengths. In fact, if the wheel base of bogie and resonance wavelengths are small then the corresponding input energy is also small. Therefore, the resonant frequencies are:

$$f = nV/(2L_s),\ n=1,2,3,... \quad (19)$$

Similarly, the anti-symmetric modes resonance wavelengths and the resonance frequencies are:

$$\lambda = 4L_s/(2n-1),\ f = (2n-1)V/4L_s,\ n=1,2,3,... \quad (20)$$

The resonance frequencies are related to the length of bogie center and speed of the vehicle. When natural frequencies are equal to the resonance frequencies, the carbody will set up resonance, the corresponding speed are called resonance speed [11]. According to Table 1, the carbody resonance speeds are shown in Fig. 2.

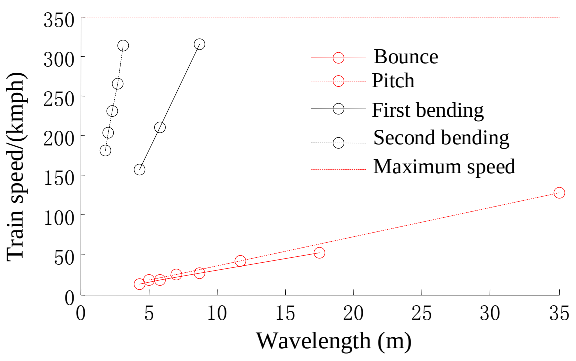

Fig. 2: Carbody resonance speed

As shown in Fig. 2, the rigid vibration resonance speeds are generally less than the vehicle running speed. The first vertical bending resonance speed is closer the vehicle running speed. It is a significant impact on the body vibration. When vehicle parameters are settled, the vehicle running speed should avoid the first bending resonance speed. The corresponding wavelengths of second and higher resonance speed are small and have less influence on vehicle. It is considered that first bending resonance vibration will be excited when bounce vibration transmissibility is maximum. Second vertical bending resonance vibration will be excited when pitch vibration transmissibility is maximum. The carbody will produce the modal resonances as long as the natural frequency is consistent with its resonant frequency, regardless of the symmetric modes and anti-symmetric modes. When the symmetric mode response is maximum, anti-symmetric mode response is zero and vice versa.

Since the acceleration power spectrum density (PSD) is related to the acceleration transmissibility, it is necessary to analyze the modal acceleration transmissibility. According to parameters in Table 1, the modal acceleration transmissibility is shown in Fig. 3. When the elastic modal vibration acceleration transmissibility is larger than that of rigid and the first vertical bending vibration, acceleration transmissibility becomes maximum. Therefore, the carbody vibration acceleration increase rapidly and ride comfort deteriorate when first vertical bending resonance happens.

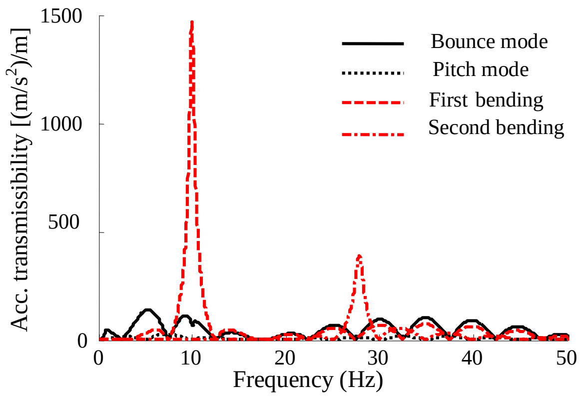

Fig. 3: Modal acceleration transmissibility

The vibration acceleration is related to track irregularities input except for the case of acceleration transmissibility. The high and low excitation track irregularity PSDs are illustrated in Fig. 4. It can be seen that the track excitation power decreases for an increase in the frequencies. So, it is important to avoid the low resonance frequencies for the carbody vibration. When considering the first four carbody modes only, using original values for the typical high speed vehicle parameters shown in Table 1 and vehicle running speed of 265 kmph (anti-symmetric modes resonance speed) and 315 kmph (symmetric modes resonance speed), the acceleration PSDs at the centre of carbody and above the centres of front and rear bogies are shown in Fig. 5. The carbody vibration is changed with frequencies and positions, each mode has different energy proportion in vibration. In 265 kmph speed, the acceleration PSDs are gradually decreased for an increase in the frequency. So the elastic vibrations have less power than rigid. Because of anti-symmetric effect, the vibration above rear bogie is more severe than the center and the front bogie. In 315 kmph, the acceleration PSD has the same vibration energy above the front and rear bogie because it is in the node of first bending vibration shape function. The center is the peak of first bending vibration shape function, the flexible vibration energy is about seven times the rigid at the center. The carbody appears to show strong elastic resonance.

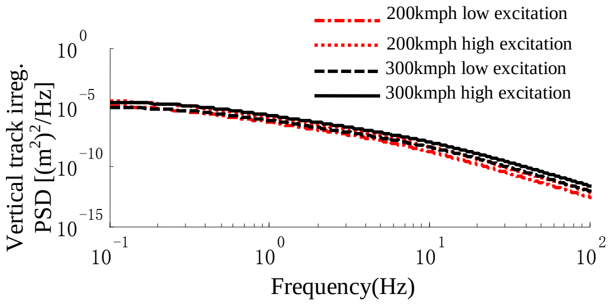

Fig. 4: High speed Track irregularity PSD

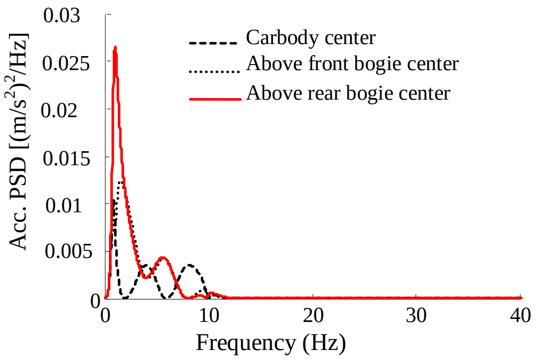

Fig. 5(a): V = 265 kmph

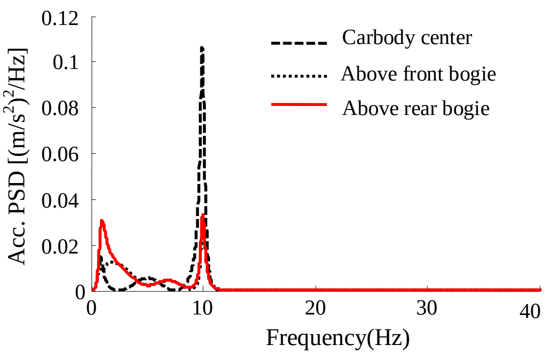

Fig. 5(b): V = 315 kmph

Fig. 5: Vertical vibration acceleration PSD of flexible carbody

The relationship between the vibration and ride quality can be measured by Sperling indices. Fig. 6 shows that the ride quality indices will increase with the increase in vehicle speed. The ride indices at the center are changed bigger than that above the bogies because of the resonance effect and filtering effect of first vertical bending vibration. The first vertical bending mode has the greatest influence on the vibration of carbody. The relations between the ride quality and the first vertical bending frequencies are illustrated in Figs. 7 and 8. Due to the filtering and resonance effects, ride indices have a drastic change with the first vertical bending frequency. It has the peak at resonance frequency and the trough at filtering frequency. Higher the vehicle speed the more dramatic change to ride quality is observed. When bending frequencies get to certain values, the ride indices reach to constant values. This value is greater when the speed is higher. This means that greater carbody stiffness is required for higher vehicle speed. Increasing bending frequency means that the mass of carbody and energy consumption are increased. For an existing vehicle, it is important to avoid the conflict of running speed and resonance speed. Because second suspension points are the node of first bending mode, it has a smaller change of ride indices above the bogies than the carbody center. When the first bending frequency is less than 8 Hz and vehicle has a high speed, the Sperling index has reached about 2.5.

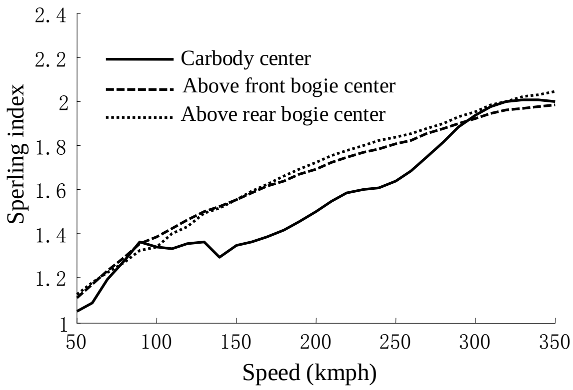

Fig. 6: Ride index vs. train speed

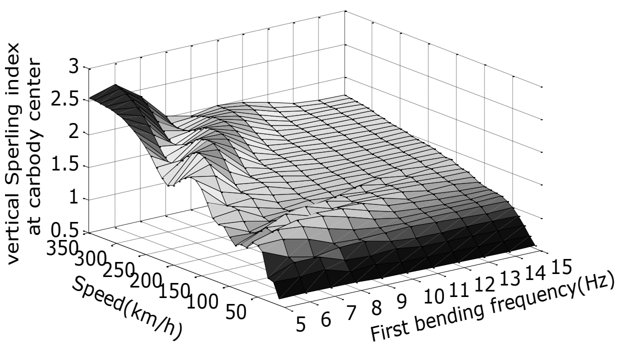

Fig. 7: Ride index at carbody center vs. Train flexibility

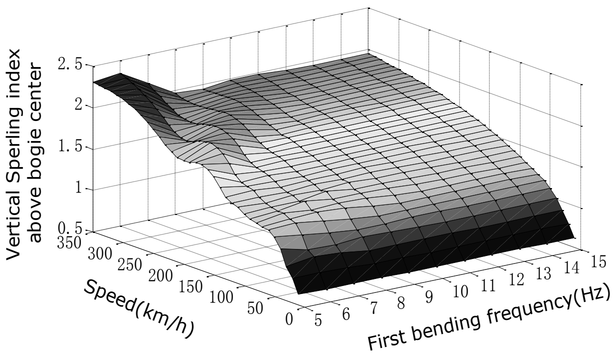

Fig. 8: Ride index above bogie center vs. Train flexibility

It is necessary to take measures to control ride quality. Usually, it can be achieved by changing the damping ratio of the structure and optimization of vehicle suspension parameters. The relationship between Sperling indices and damping ratio are illustrated and evaluated in Fig. 9 when the vehicle speed is 300 kmph. Results show that when damping ratio increases from 0.015 to 0.15 ride index can be decreased by about 13%. Increasing the damping ratio can significantly reduce the vibration of carbody. The structure surface damping layers process, passive or active damping control measures can be taken to improve the carbody damping [12-14]. Vertical suspension parameters have an important influence on ride quality. The vertical stiffness is determined by the vehicle structure. So damping coefficients change can be taken to improve ride quality. Figs. 10 and 11 illustrate the ride quality changes with the damping coefficients and speed. Higher primary damping reduces the rigid and flexible vibration. Higher primary damping may deteriorate the maximum dynamic wheel-rail forces. So appropriate damping is helpful to improve the ride comfort.

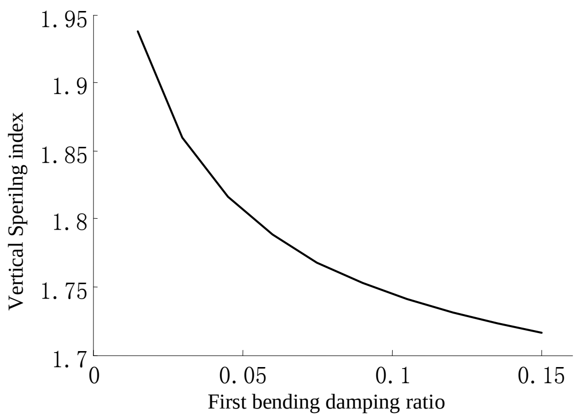

Fig. 9: Effect of carbody structural damping on ride index

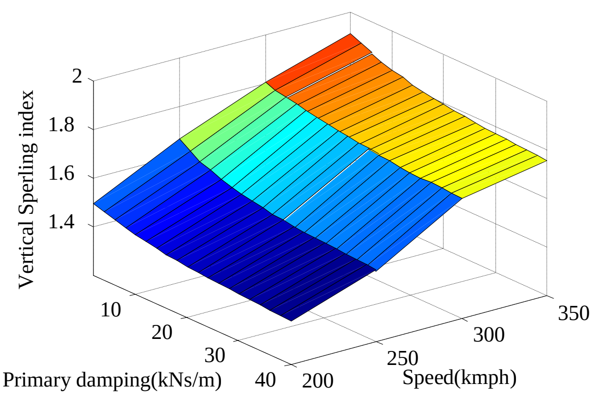

Fig. 10: Effect of vertical primary damping on ride index

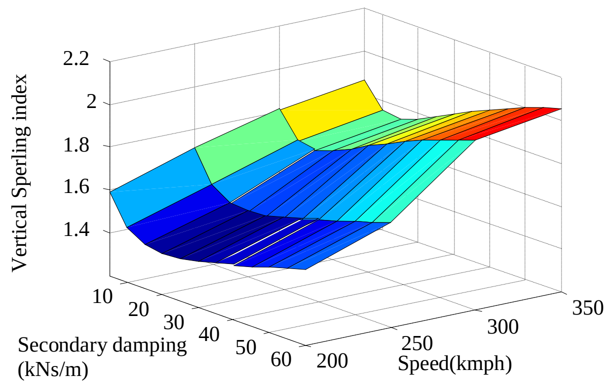

Fig. 11: Effect of vertical secondary damping on ride index

Secondary damping has an optimal value, higher the vehicle speed, smaller the damping is needed. In Fig. 11, the optimum values of secondary damping coefficients are 20 kNs/m and 15 kNs/m for 200 kmph and 300 kmph respectively. It is because when the speed is high, excitation frequency is high, secondary vertical damping should decrease appropriately to dissipate the vibration.

4. Conclusions

The modal vibration has the resonance effect and filtering effect, in particular track wavelength, symmetric modes vibration is zero and anti-symmetric modes vibration is the strongest and vice versa. Each mode has its corresponding resonance frequency. First bending mode acceleration transmissibility is maximum and has the largest contribution to vibration. The first bending resonance speed has a dramatic impact on ride indices. When this speed is equal to the vehicle speed, the elastic resonance happens. So it is necessary to avoid this situation. The rigid resonance speed is lower than running speed and has a little impact on the ride quality. A lower bending frequency can deteriorate the vehicle ride quality. So when running speed of a vehicle is higher larger the bending frequency is required. Improving the primary damping and the structure damping appropriately reduces the secondary damping and thereby vehicle ride quality can be improved.

REFERENCES:

[1] H. Suzuki. 1998. Research trends on riding comfort evaluation in Japan, *Proc. IMechE Part F: J. Rail & Rapid Transit*, 212(1), 61-72. http://dx.doi.org/10.1243/0954409981530689.

[2] P.F. Carlbom. 2001. Combining MBS with FEM for rail vehicle dynamics analysis, *J. Multibody System Dynamics*, 6(3), 291-300. http://dx.doi.org/10.1023/A:1012072405882.

[3] G. Diana, F. Cheli, A. Collina, R. Corradi and S. Melzi. 2002. The development of a numerical model for railway vehicles comfort assessment through comparison with experimental measurements, *J. Vehicle System Dynamics*, 38(3), 165-183. http://dx.doi.org/10.1076/vesd.38.3.165.8287.

[4] D. Gong, J.S. Zhou and W.J. Sun. 2013. On the resonant vibration of a flexible railway car body and its suppression with a dynamic vibration absorber, *J. Vibration & Control*, 19(5), 649-657. http://dx.doi.org/10.1177/1077546312437435.

[5] J.S. Zhou, D. Gong, W.J. Sun and L.H. Ren. 2009. Influence of vertical elasticity of carbody of railway passenger vehicles on ride quality, *J. China Railway Society*, 31(2), 32-37.

[6] J. Zhou, R. Goodall, L. Ren and H. Zhang. 2009. Influences of car body vertical flexibility on ride quality of passenger railway vehicles, *Proc. IMechE Part F: J. Rail & Rapid Transit*, 223(5), 461-471. http://dx.doi.org/10.1243/09544097JRRT272.

[7] J. Zeng and R. Lou. 2007. Vibration analysis of railway passenger car systems by considering flexible carbody effect, *J. China Railway Society*, 29(6), 19-25.

[8] C.H. Huang, J. Zeng, P.B. Wu and R. Luo. 2010. Study on carbody flexible vibration reduction for railway passenger carriage, *Engg. Mechanics*, 27(12), 250-256.

[9] Y. Suzuki and K. Akutsu. 1990. Theoretical analysis of flexural vibration of car body, *Railway Technical Research Institute*, Quarterly Reports, 31(1).

[10] V. Cossalter, A. Doria, S. Garbin and R. Lot. 2006. Frequency-domain method for evaluating the ride comfort of a motorcycle, *Vehicle System Dynamics*, 44(4), 339-355. http://dx.doi.org/10.1080/00423110500420712.

[11] F. Cheli and R. Corradi. 2011. On rail vehicle vibrations induced by track unevenness, Analysis of the excitation mechanism, *J. Sound & Vibration*, 330(15), 3744-3765. http://dx.doi.org/10.1016/j.jsv.2011.02.025.

[12] C.H. Huang and J. Zeng. 2010. Flexural vibration suppression of car body for high-speed passenger car based on constrained damping layers, *J. Traffic & Transportation Engg.*, 10(1), 36-42.

[13] M. Kozek, C. Benatzky, A. Schirrer and A. Stribersky. 2011. Vibration damping of a flexible car body structure using piezo-stack actuators, *Control Engg. Practice*, 19(3), 298-310.

[14] S. Bruni, R. Goodall, T.X. Mei and H. Tsunashima. 2007. Control and monitoring for railway vehicle dynamics, *Vehicle System Dynamics*, 45(7-8), 743-779. http://dx.doi.org/10.1080/00423110701426690.